

Neasta et al.

Supplemental Material

Methods for mass spectrometry identification of proteins:

In-gel protein digestion

The whole lanes (IgG versus RACK1) of interest were manually excised and cut into small pieces from a representative gel. The gel pieces were washed and dried under vacuum. Proteins were reduced and alkylated by rehydration with 10 mM dithiothreitol in 25 mM NH_4HCO_3 for 45 min at 56°C followed by incubation in 55 mM iodoacetamide in 25 mM NH_4HCO_3 for 30 min at room temperature in the dark. Gel pieces were then washed with 25 mM NH_4HCO_3 and acetonitrile (ACN) and then dried in a vacuum centrifuge. Gel pieces were rehydrated in a sufficient covering volume of modified trypsin solution (12.5 ng/ μl in 25 mM NH_4HCO_3) and incubated overnight at 37°C. Peptides were extracted twice for 15 min with shaking using 50% ACN/ 0.1% trifluoroacetic acid (TFA). The peptide mixture was concentrated in a vacuum centrifuge to a final volume of about 10 μl and were manually desalted using C18 Ziptips (Millipore). Peptides were then eluted with 50% ACN/0.1% TFA and solvent was removed under vacuum. Peptides were reconstituted in 5 μl of 0.1% TFA and 1 μl was used for liquid chromatography (LC) MS/MS analysis.

NanoLC-ESI-Q-TOF MS/MS analysis

Mixtures of proteolytic peptides were on-line separated by nanoLC utilizing Eksigent 2D LC NanoLC System (Eksigent/ Applied Biosystems Sciex) interfaced with QStar XL

Neasta et al.

mass spectrometer (Applied Biosystems Sciex) equipped with a Protana nanospray source. External calibration was performed in MS/MS mode using fragment ions of Glu1-fibrinopeptide as references. LC Packings Pepmap C18 trap column (300 μm i.d., 5mm length, 300 \AA pore size, 5 μm bead size) and a column (75 μm i.d., 15 cm length) self-packed with Jupiter Proteo C12 end-capped material (90 \AA pore size, 4 μm bead size) were used for desalting and reversed phase peptide separation, respectively. A 40 min linear gradient from 2% B to 50% B in A was run at 250 nl/min flow rate, utilizing solvents A: 2% ACN in 0.1% formic acid and B: 80% ACN in 0.08% formic acid. Precursor ion selection employed an automated routine (IDA, Analyst QS 1.1. AB Sciex) that consisted of a series of one survey MS scan (1 s, m/z 400-1600, detection threshold 3 counts) and two MS/MS scans (2 s, m/z 80-1600) employing “enhance all” mode. The following IDA parameters were used: minimum signal intensity = 10 counts; charge state 2 or 3; dynamic exclusion of former target ion: mass tolerance 350 ppm, isotopes excluded, exclusion time 40 s. Nitrogen served as collision gas and collision energy was automatically adjusted depending on the size and charge state of the precursor ion.

Protein database search

ProteinPilotTM Software 4.0 software that utilizes the ParagonTM Algorithm (Applied Biosystems Sciex) was used for peak detection, mass peak list generation and database searches. Uniprot UniProtKB/Swiss-Prot Protein Knowledgebase release 57.0 of March 24, 2009, category mammalia (72729 protein sequences) was interrogated. Paragon search algorithm does not limit the search space to specific variable modifications, mass tolerances and number of missed cleavages. The following search parameters were used:

Neasta et al.

trypsin for enzyme specificity, carbamidomethylation as a fixed modification of cysteine residues and search effort of “thorough”. Special Factors were set to gel-based ID and urea denaturation. ID Focus was set to biological modifications and amino acid substitutions. Protein identifications based on multiple peptides were accepted using a cut-off score of 1.69897 that represented $\geq 98\%$ confidence. However, in cases of identities based on a single peptide, a cut-off score of 2.0 representing $\geq 99\%$ confidence was employed. No estimate of false positive rate was performed due to the relatively small datasets generated in this study.

Supplemental figure legends:

Figure S1: Evidence for mass spectrometry-based protein identification of 14-3-3 ζ and 14-3-3 θ . *A* Table shows the characteristics of the assigned peptides leading to the identification of 14-3-3 ζ and 14-3-3 θ (MW stands for molecular weight and Theor for theoretical). *Peptide modified with carbamidomethyl at C and missed cleavage at R. **When a peptide is common for multiple proteins, its score contributes only to the top hit protein, in this case to 14-3-3 θ . *B* MS/MS spectrum of the peptide ²⁸SVTEQGAELSNEER⁴¹ derived from 14-3-3 ζ . Peaks corresponding to *b* and *y* product ion series are annotated in green and red, respectively. Table shows theoretical *m/z* values of product ions: the observed ions are shown in bold against green background.

Figure S2: Activation of the cAMP pathway does not change the global amount of RACK1 and 14-3-3 ζ . SHSY5Y cells were treated with 10 μ M of FSK or vehicle for the

Neasta et al.

indicated duration. Cells were lysed in radioimmunoprecipitation assay buffer (RIPA) buffer and the same amount of proteins was resolved by SDS-PAGE. The presence of RACK1 and 14-3-3 ζ and actin was determined by western blot analysis. One-way ANOVA did not detect any effect of the treatment neither for RACK1 [$F_{(2,6)} = 0.77$, $P = 0.503$] nor for 14-3-3 ζ [$F_{(2,6)} = 1.63$, $P = 0.273$], $n=3$. Histogram depicts the mean ratio of RACK1 or 14-3-3 ζ to actin expressed in percentage of control \pm SEM.

Figure S3: *In vitro* digestion of recombinant GST-14-3-3 θ by thrombin. Recombinant GST-14-3-3 θ was expressed in *Escherichia coli*, immobilized on a sepharose column and submitted to thrombin digestion for 18h. Digested proteins were recovered in the mobile phase, resolved by SDS-PAGE and proteins were stained with colloidal Coomassie blue.

Figure S4: Peptide array analysis of the full RACK1 sequence for identification of potential 14-3-3 ζ binding loci. An array of immobilized 18-mer peptide spots frameshifted in 3-residue increments and spanning the entire length of RACK1 was probed with GST-14-3-3 ζ . Binding of 14-3-3 ζ was detected (dark spots) by immunoblotting against GST.

Figure S5: Alanine scanning array analysis of RACK1 peptide 59. Arrays in which the 18 amino acids in RACK1-derived 18-mer peptide 59, defined in Fig. 4B, was sequentially substituted with alanine and probed using GST-14-3-3 ζ . The binding of GST-14-3-3 ζ to each alanine-substituted RACK1 peptide was detected by immunoblotting

Neasta et al.

against GST and quantified by densitometry, presented here as a percentage relative to the binding of GST-14-3-3 ζ to the unsubstituted parent peptides as controls (Co).

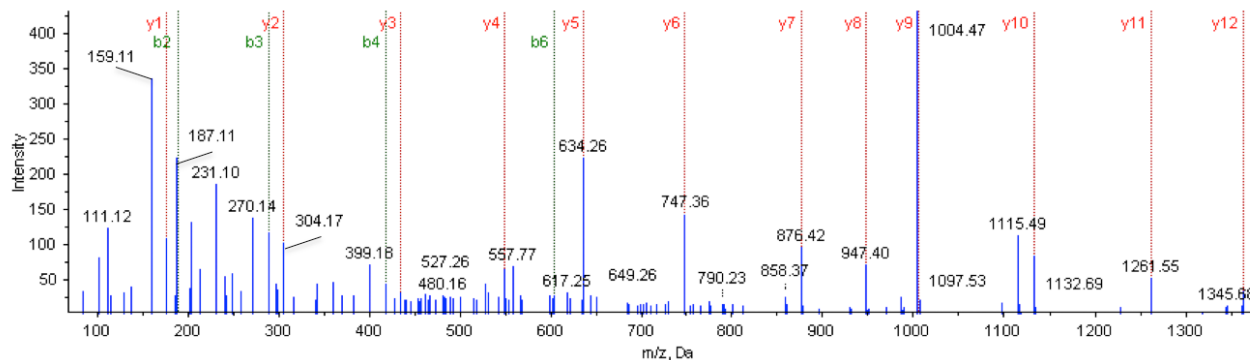
Figure S1

A

Peptide scores assigned to this ID	Sum of all matching peptide scores	% Protein sequence coverage (peptide confidence >95%)	Entry name	Swiss-Prot Accession number	Protein name	Peptide contribution to protein score	Confidence of peptide match	Peptide Sequence	Mass Error (ppm)	MW (Da)	m/z	Theor MW (Da)	Theor m/z	Theor z
6	6	14,7	1433T_HUMAN	P27348	14-3-3 protein theta	2	99,000001	AVTEQGAELSNEER	0,4	1531,7120	766,863	1531,7114	766,863	2
						2	99,000001	DSTLIMQLLR	-2,2	1188,6511	595,333	1188,6537	595,334	2
						2	99,000001	*YLAEVACGDDRK	26,5	1395,6823	466,235	1395,6453	466,222	3
2	4	9,8	1433Z_HUMAN	P63104	14-3-3 protein zeta	2	99,000001	SVTEQGAELSNEER	1,8	1547,7091	774,862	1547,7063	774,860	2
						0	99,000001	**DSTLIMQLLR	-2,2	1188,6511	595,333	1188,6537	595,334	2

B

(MK²⁷)²⁸SVTEQGAELSNEER⁴¹ (NL⁴³)



Residue / Fragment Ion	N-term ion #	a	b	b-H2O	y	y-H2O	y-NH3	C-term ion #
S	1	60.04	88.04	70.03	1548.71	1530.70	1531.69	14
V	2	159.11	187.11	169.10	1461.68	1443.67	1444.66	13
T	3	260.16	288.16	270.14	1362.61	1344.60	1345.59	12
E	4	389.20	417.20	399.19	1261.57	1243.55	1244.54	11
Q	5	517.26	545.26	527.25	1132.52	1114.51	1115.50	10
G	6	574.28	602.28	584.27	1004.46	986.45	987.44	9
A	7	645.32	673.32	655.30	947.44	929.43	930.42	8
E	8	774.36	802.36	784.35	876.41	858.40	859.38	7
L	9	887.45	915.44	897.43	747.36	729.35	730.34	6
S	10	974.48	1002.47	984.46	634.28	616.27	617.25	5
N	11	1088.52	1116.52	1098.51	547.25	529.24	530.22	4
E	12	1217.56	1245.56	1227.55	433.20	415.19	416.18	3
E	13	1346.61	1374.60	1356.59	304.16	286.15	287.14	2
R	14	1502.71	1530.70	1512.69	175.12	157.11	158.09	1

Figure S2

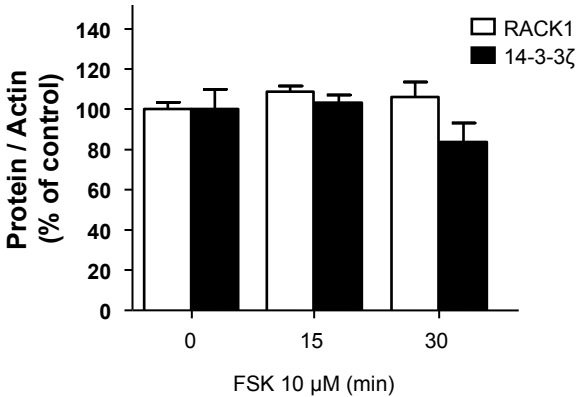
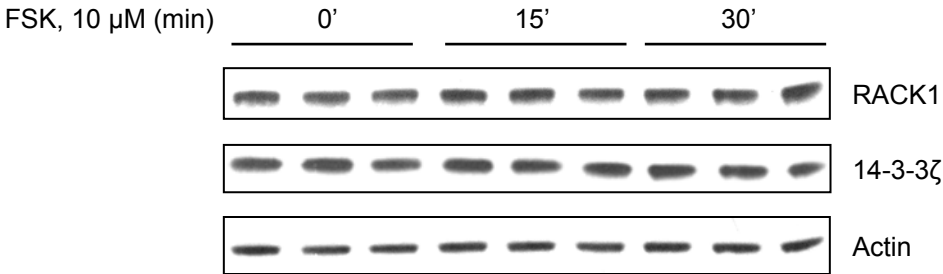


Figure S3

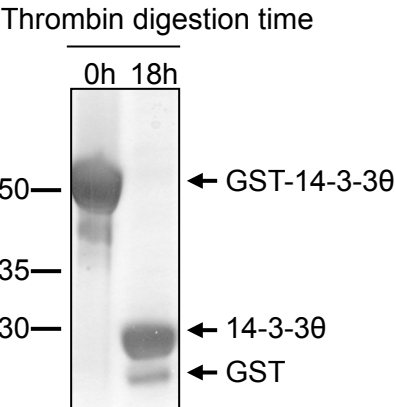


Figure S4

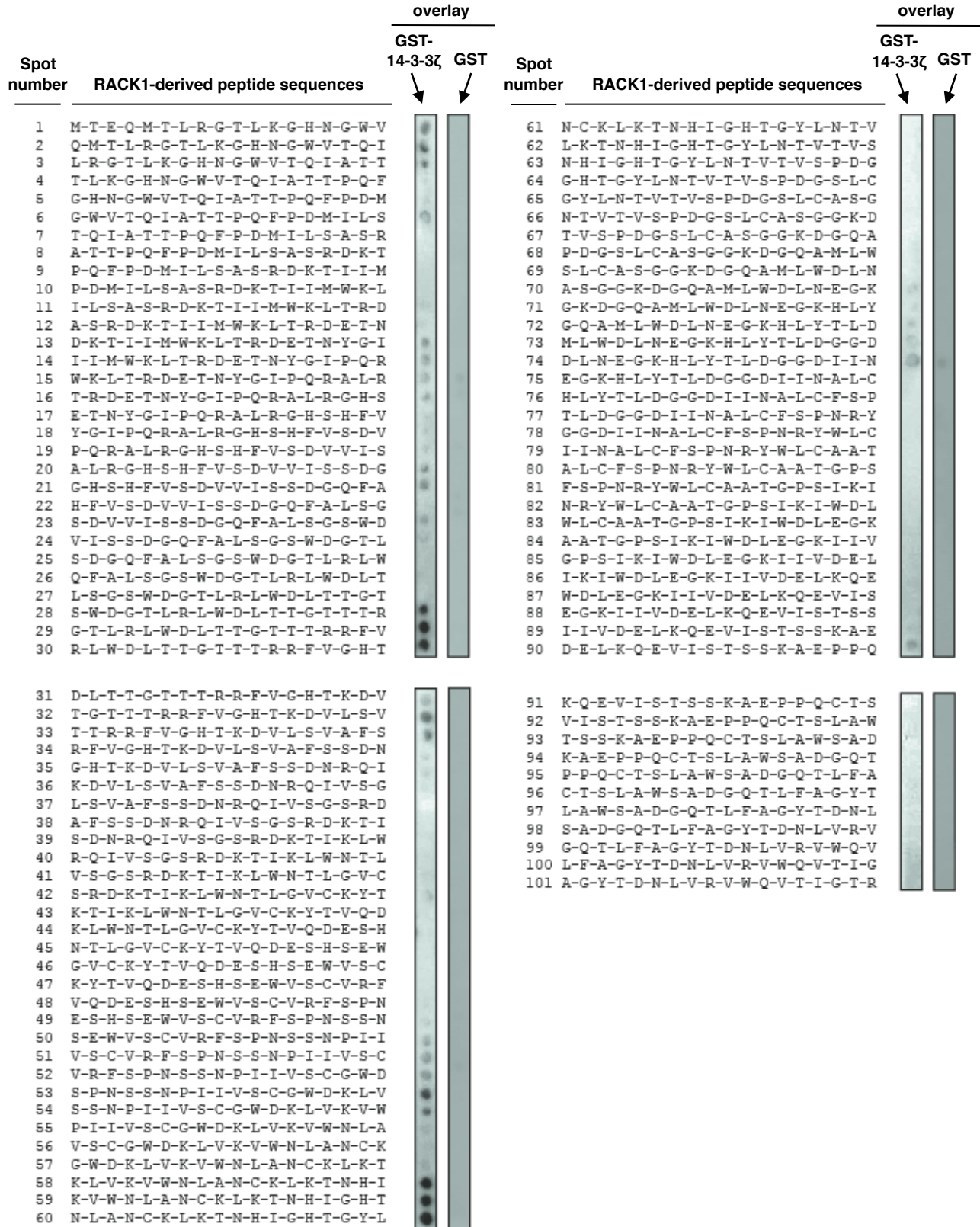


Figure S5

